Journal of Applied Electrochemistry **30**: 491–498, 2000.
© 2000 *Kluwer Academic Publishers. Printed in the Netherlands.*

Effect of oxygen and titanium contents on the stability of nanocrystalline Ti–Ru–Fe–O cathode materials for chlorate electrolysis

L. ROUÉ[1], M.-E. BONNEAU[1], D. GUAY[1,*], M. BLOUIN[2] and R. SCHULZ[2]
[1]*INRS-Énergie et Matériaux, 1650 Blvd. Lionel-Boulet, C.P. 1020, Varennes, Québec, Canada, J3X 1S2;*
[2]*Technologies Émergentes de production et de stockage, Institut de recherche d'Hydro-Québec, 1800 Blvd. Lionel-Boulet, C.P. 1000, Varennes, Québec, Canada, J3X 1S1*
*(*author for correspondence; e-mail: guay@inrs-ener.uquebec.ca)*

Received 20 April 1999; accepted in revised form 30 October 1999

Key words: ball milling, chlorate electrolysis, electrocatalysis, hydrogen evolution, nanocrystalline

Abstract

Electrodes made from nanocrystalline Ti:Ru:Fe $(2-y:1+y/2:1+y/2)$, with y varying from 0 to 1 by step of 0.25, and Ti:Ru:Fe:O (2:1:1:w), with w varying from 0 to 2 by step of 0.5, were prepared and tested as activated cathodes for the hydrogen evolution reaction in typical chlorate electrolysis conditions. These electrodes were subjected to an accelerated aging test, consisting of a succession of cycles of hydrogen discharge (HER) and open-circuit (OCP) conditions. In addition to monitoring the cathodic overpotential value during the aging test, visual inspection and mass loss measurements were performed on the electrodes at the end of the test to assess their stability. In the case of Ti:Ru:Fe (2:1:1), a large increase of the cathodic overpotential value is observed after 20 cycles. Adding O to the formulation causes a remarkable improvement of the long-term stability of the electrodes. As little as [O] = 10 at.% in nanocrystalline Ti:Ru:Fe:O (2:1:1:w) materials is sufficient for the electrode to show absolutely no sign of degradation after 50 cycles of HER/OCP, the longest accelerated test conducted. Adding more O to the formulation of the material does not lead to further stability improvement. A better stability under the conditions of the accelerated aging test can also be observed for nanocrystalline Ti:Ru:Fe $(2-y:1+y/2:1+y/2)$ materials with $y > 0$. In that case however, the level of improvement is dependent on the value of y. The best results are obtained for $y = 0.75$. A hypothesis is proposed to explain the improved stability obtained by lowering the Ti content and/or by adding O. The similarity and difference between both ways of improving the stability of the nanocrystalline Ti:Ru:Fe materials are also discussed.

1. Introduction

The first step in the formation of sodium chlorate is the anodic discharge of chloride ions to chlorine, with the concomitant hydrogen discharge reaction at the cathode. Sodium chlorate is then formed from chlorine through a series of chemical reactions. Approximately 70% of the production costs of sodium chlorate are associated with the consumption of electrical energy. The overall efficiency of the electrolysis cell depends on several factors [1], of which the choice of the electrode materials for the anodic and cathodic reactions is of utmost importance.

Since the introduction of the Dimensionally Stable Anode (DSA®) in the chlorate industry, not much energy savings can be performed by developing new anode materials. DSA electrodes give very low anodic overpotential, typically 40 mV at 250 mA cm^{-2}. On the other hand, the total cathodic overpotential of the steel cathodes usually used in the chlorate industry is about -800 mV at -250 mA cm^{-2}. This constitutes the main electrochemical energy loss in the production of sodium chlorate.

Numerous electrode materials have been developed to catalyze the hydrogen evolution reaction [2]. However, most of these materials are not suited for application in the chlorate industry. Actually, a viable chlorate cathode must ideally meet the following requirements: (i) low H_2 evolution overpotential; (ii) inactivity towards chemical decomposition of hypochlorite; (iii) no interference with the selectivity of the dynamic chromium hydroxide film, i.e. the rate of hypochlorite and chlorate reduction at the cathode must be low; (iv) stability under open circuit condition in hot chlorate liquor; (v) high level of resistance towards hydrogen embrittlement; (vi) lifetime of several years, typically 6 years; (vii) ability to withstand periodic cleaning with 5–10% HCl; (viii) low cost. Obviously, this long list of criteria reduces the potential candidates.

We have recently shown that considerable improvement in the electrocatalytic activity for the hydrogen

evolution reaction (HER) in typical chlorate electrolysis conditions can be obtained by using cathodes based on nanocrystalline Ti–Ru–Fe prepared by high energy ball milling [3]. Indeed, using such electrode material, a reduction of the cathodic overpotential at -250 mA cm^{-2} of about 250 mV is observed compared to a steel electrode.

However, during prolonged electrolysis, a nanocrystalline Ti:Ru:Fe (2:1:1) electrode suffers from decrepitation and loss of material, resulting in an increase of the cathodic overpotential and, eventually, in the rupture of the electrode [4]. This limitation can be overcome and the structural integrity of the electrode can be dramatically improved by the addition of oxygen. For example, the cathodic overpotential of electrodes made from nanocrystalline materials obtained through milling of Ti:Ru:Fe:O (2:1:1:2) does not vary over a period of 1000 h (the longest test conducted so far), nor does the electrode show any sign of degradation after this prolonged test [5]. In comparison, the cathodic overpotential of an electrode made from the O-free material starts to increase (becoming more cathodic) after only $\sim$100 h [4]. Obviously, oxygen has a beneficial effect on the stability of the electrode.

It has been shown previously that prolonged milling of Ti:Ru:Fe (2:1:1) produces a nanocrystalline alloy made almost exclusively (97 wt.%) of a B2 cubic phase (cP2-CsCl), whose composition is Ti_2RuFe, with only a small fraction (3 wt.%) of bcc iron [3, 6]. In contrast, the materials obtained after extensive milling of Ti:Ru:Fe:O (2:1:1:2) is multi-phased, comprising $\sim$60 wt.% of a B2 cubic phase, $\sim$30 wt.% of titanium oxides, the remaining 10 wt.% being either Ru or Fe [6, 7, 8]. In Ti:Ru:Fe:O (2:1:1:2), the Ti/O ratio is fixed at unity by the initial composition of the powder. Thus, the formation of the more stable titanium oxide phases during milling affects the amount of Ti atoms which can be involved in the formation of the less stable B2 cubic phase. A detailed analysis of both X-ray and neutron diffraction data of a series of nanocrystalline Ti:Ru:Fe:O (2:1:1:w), where w was varied from 0 to 2 was reported previously [6]. In that study, it was demonstrated that the presence of oxygen in the powder mixture leads to the formation of Ti oxides and a Ti-depleted B2 cubic phase, $Ti_{2-x}Ru_{1+y}Fe_{1+z}$, with x being as large as 0.74 when $w = 1.5$.

A first hint at the reasons underlying the improved stability by the addition of O comes from the markedly different behavior between the oxygen-free and oxygen containing materials when they are subjected to a succession of cycles of hydrogen discharge and open circuit conditions. In experiments where the hydrogen discharge and open circuit conditions last ten minutes each, some material starts to fall from the surface of the electrode prepared from nanocrystalline Ti:Ru:Fe (2:1:1) at the tenth cycle, leading to a marked increase of the cathodic overpotential at the twentieth cycle [4]. In contrast, there is no change in the cathodic overpotential of electrodes prepared from Ti:Ru:Fe:O (2:1:1:1) even after fifty cycles, nor does the surface of the electrode show any sign of material lost [4]. To explain this different behavior, it was hypothesized: (i) that hydrogen is able to dissolve into the structure of the O-free nanocrystalline material during hydrogen discharge, while it is released from the electrode under open circuit conditions, and (ii) that the dissolution/release of hydrogen into/from the material could be at the origin of stresses leading to the decrepitation and rupture of the electrode. As a corollary, we assume that the addition of oxygen to nanocrystalline Ti:Ru:Fe somehow modifies the structure and phase composition of the milled compound, reducing or preventing hydrogen absorption into the material.

Recently, this hypothesis found strong support when it was shown by *in situ* X-ray diffraction that there is a sizeable increase in the volume of the unit cell of the B2 phase of nanocrystalline Ti:Ru:Fe (2:1:1) when this material is exposed to hydrogen at high pressure [9]. This increase in the unit cell upon hydrogen exposure is totally reversible, the diffraction peaks returning to their original positions when hydrogen is removed from the reaction cell. In the same experiment, it was also shown that the volume expansion of Ti-depleted cubic phases was much less than that of Ti_2RuFe for the same hydrogen pressure [9]. At first sight, this reinforces the idea that the improved stability of nanocrystalline Ti:Ru:Fe:O (2:1:1:2) arises as a consequence of a modification of the intrinsic hydrogen sorption properties of the Ti-depleted B2 cubic phase, whose formation is favored by the presence of O. If this hypothesis holds true, the long-term stability of electrodes made from nanocrystalline Ti:Ru:Fe $(2-y:1+y/2:1+y/2)$, whose major component is the Ti-depleted B2 phase, should compare with that of nanocrystalline Ti:Ru:Fe:O. On the other hand, if electrodes made from Ti-depleted B2 phase do not show any improvement compared to Ti_2RuFe, this tends to demonstrate the crucial role played by (substoichiometric) titanium oxide phases in preventing hydriding [10].

In the first part of this work, the long-term stability of nanocrystalline Ti:Ru:Fe:O (2:1:1:w) compounds prepared by high energy ball milling will be determined as a function of the oxygen content, for w ranging from 0.0 to 2.0 by steps of 0.5. This will be done by using an accelerated aging test, whereby the electrode is subjected to a series of alternating cycles of hydrogen discharge and open circuit conditions. This test has demonstrated its relevance to assess the long-term stability of cathodes in chlorate electrolysis conditions [4]. In the second part, the long-term stability of nanocrystalline Ti:Ru:Fe $(2-y:1+y/2:1+y/2)$ compounds will be determined as a function of the titanium content, for y ranging from 0.00 to 1.00 by steps of 0.25. It will be shown that the long-term stability of these materials is highly dependent on the values of w and y, determining the O and Ti content, respectively. The reasons underlying the improved stability by an increase of O or a decrease of Ti will be outlined.

2. Experimental

2.1. *Preparation of samples*

Samples were made by high-energy ball milling using a SPEX 8000 mixer/mill apparatus. From previous experiments [3], the milling time was set at 40 h. In all cases, steel balls and vials were used. The vial has a diameter of 38.1 mm and a length of 47.6 mm. Three balls were used, one with a diameter of 14 mm and two with a diameter of 11 mm. The ball to powder ratio was about 4:1. The vial was always filled with argon to prevent oxidation and nitridation reactions.

Pure Ti, TiO, Ru, Fe and Fe_2O_3 (purity 99.0% or higher) powders were used as starting materials. The following nanocrystalline Ti:Ru:Fe:O samples were prepared: (i) (2:1:1:w), with w varying from 0.0 to 2.0 by step of 0.5, and Ti:Ru:Fe $(2-y:1+y/2:1+y/2)$, with y varying from 0.00 to 1.00 by step of 0.25.

2.2. *Chemical and physical analyses*

The oxygen and nitrogen contents of the powders after ball milling were measured with a TC-136 oxygen/nitrogen detector from LECO. The nitrogen and oxygen contents when no oxide is added to the initial powder mixture were less than 0.1 wt.% and 1.0 wt.%, respectively. In the cases where oxides were deliberately added, the nitrogen was always less than 0.1 wt.%, while oxygen was close to the expected value (within 1 wt.%).

X-ray diffraction was performed using a PHILIPS PW3040 diffractometer with Cu K_α radiation. Structural parameters were extracted from the X-ray spectra by performing Rietveld refinement analyses using the GSAS software [11].

Scanning electron microscopy (SEM) observations of the morphology of the electrodes were made using a HITACHI S-570 microscope operating at 15 kV. Chemical analyses were performed by energy dispersive X-ray (EDX) analysis. The samples after electrolysis were cleaned with deionized water at 70 °C for 30 min prior to analysis.

Atomic force microscopy (AFM) observations of the morphology of the material surface were performed with a Nanoscope III (Digital Instruments) in contact mode using commercially available Si_3N_4 tips.

2.3. *Electrochemical measurements*

The working electrode was a pellet made by cold pressing the powders with a load of 10000 kg cm^{-2} for 10 min into a stainless steel dye of 16 mm in diameter. Pellets were made from 0.3 g of powder deposited on 1.0 g titanium powder. The pellets were mounted on a glass tube with resin. Electrical contact was made at the back of the electrode (titanium side) by an electrical wire with silver epoxy bonding. The geometric area of the working electrode exposed to the electrolyte was 2 cm^2. A 50 cm^2 DSA® was used as the counter electrode and all potentials were measured against a saturated calomel electrode (SCE) reference, using a Luggin capillary set close to the surface of the working electrode.

The electrochemical experiments were performed in a double wall glass cell with a capacity of about one-liter. All experiments were performed at 70 °C. The composition of the electrolyte was that used in the chlorate industry ($NaClO_3$:550 g l^{-1}, NaCl:110 g l^{-1}, $Na_2Cr_2O_7$: 3 g l^{-1}, NaClO:1 g l^{-1}). The pH was maintained at about 6.5 by regular addition of 10 M HCl. The electrolytic solution was changed periodically.

The electrochemical measurements were performed using a SI 1287 Solartron potentiostat-galvanostat controlled by CorrWare software. The ohmic drop was determined by impedance measurements (using SI1255 Solartron HF frequency response analyzer controlled by Zplot software and connected to the SI 1287 Solartron potentiostat-galvanostat). The overpotential at −250 mA cm^{-2} for the HER was calculated from the potential values after correction for the ohmic drop and the reversible potential for HER was taken as −681 mV versus SCE. Accelerated aging tests were performed in the chlorate electrolyte by submitting the electrodes to a succession of cycles of hydrogen discharge (−250 mA cm^{-2}, 10 min) and open circuit potential (10 min).

3. Results

3.1. *Effect of the O content*

3.1.1. *Structural investigations*

The X-ray diffraction patterns of nanocrystalline Ti:Ru:Fe:O (2:1:1:w), with w varying from 0.0 to 2.0 by steps of 0.5 are presented in Figure 1. A detailed analysis of these patterns using Rietveld refinement of X-ray diffraction data [7, 8] and a simultaneous analysis of X-ray and neutron diffraction data [6] was presented previously.

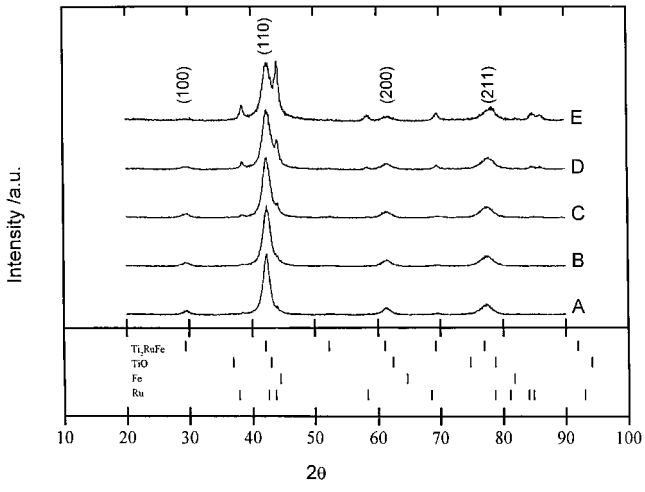

Fig. 1. X-ray diffraction patterns of nanocrystalline Ti:Ru:Fe:O (2:1:1:w): (A) $w = 0.0$, (B) $w = 0.5$, (C) $w = 1.0$, (D) $w = 1.5$, and (E) $w = 2.0$.

The information obtained from these analyses are summarized in the upper half of Table 1. In the absence of oxygen, milling of Ti:Ru:Fe (2:1:1) leads to the formation of a B2 cubic structure whose stoichiometry is close to Ti_2RuFe. In this case, the milled material is made almost exclusively of this Ti_2RuFe cubic phase (97 wt.%), the remaining 3 wt.% being accounted for by the presence of a small amount of bcc Fe. The peaks belonging to the B2 structure are indexed in Figure 1.

When oxygen is present, it reacts with Ti to form various titanium oxides (see Figure 1). This creates a depletion of Ti on the 1a site of the B2 phase, which is preferentially filled with Fe [6]. There are also some amounts of Ru and Fe. The phase proportions of Ti oxides, Ru and Fe increase while that of $Ti_{2-x}Ru_{1+y}Fe_{1+z}$ decreases with the oxygen content. The nanocrystalline Ti:Ru:Fe:O (2:1:1:*w*) is indeed a multi-phased system.

3.1.2. *Morphological and chemical investigations*

The scanning electron microscopy (SEM) micrograph of the surface of nanocrystalline Ti:Ru:Fe:O (2:1:1:2) is shown in Figure 2. The surface morphologies of the other samples are very similar to that of Figure 2. Irregular particles with a size on the order of one micrometer are present. The relatively large particle size of the powder despite the nanocrystalline nature of the material can be explain by the cold welding of the fragmented powders during the milling operation. This is confirmed by the atomic force microscopy (AFM) image of the same material shown in Figure 3, where each particle seems to be formed by the agglomeration of many small grains welded together. The size of the smallest structure observed in Figure 3 is ~50 nm, which is close to the radius of the tip used to image the surface of the sample. The intrinsic limitation of AFM in imaging densely packed objects with dimensions approaching or smaller than the tip radius is well known, and the characteristic length determined above must be viewed as an upper limit to the size of the crystallite making up the particle.

The chemical compositions of all samples, as determined by EDX analysis, are quite close to that expected from the nominal composition of the powder mixtures. For all samples, a very slight iron enrichment is systematically observed however (about 5 at.% more Fe than expected), most probably arising from the erosion of the steel balls and container during the milling process. This finding is consistent with the presence of an unreacted bcc Fe phase in some XRD

Table 1. Structural parameters of the milled powders

Nominal composition	Phase	Lattice parameters		Crystallite size /nm	Phase concentration /wt.%
		a/(Å)	c/(Å)		
Ti:Ru:Fe:O					
2:1:1:0	$Ti_{1.90}Ru_{1.05}Fe_{1.05}$	3.031		7	97
	Fe	2.873		11	3
2:1:1:1/2	$Ti_{1.46}Ru_{1.38}Fe_{1.16}$	3.024		6	85
	TiO_x	4.204		8	6
	Ru	2.693	4.331	8	3
	Fe	2.880		8	6
2:1:1:1	$Ti_{1.50}Ru_{1.26}Fe_{1.24}$	3.031		6	72
	TiO_x	4.205		5	14
	Ru	2.736	4.243	11	6
	Fe	2.881		5	8
2:1:1:3/2	$Ti_{1.26}Ru_{1.22}Fe_{1.52}$	3.040		11	73
	TiO_x	4.169		54	17
	Ru	2.690	4.256	33	10
2:1:1:2	B2[†]	3.029		10	59
	TiO_x	4.126		28	31
	Ru	2.709	4.219	35	10
Ti:Ru:Fe					
2:1:1	$Ti_{1.90}Ru_{1.05}Fe_{1.05}$	3.031		7	97
	Fe	2.873		11	3
1.75:1.175:1.175	$Ti_{1.59}Ru_{0.89}Fe_{1.52}$	3.023		9	92
	Ru	2.711	4.269	22	4
	Fe	2.878		8	4
1.5:1.25:1.25	$Ti_{1.37}Ru_{0.86}Fe_{1.77}$	3.020		10	92
	Ru	2.709	4.269	20	4
	Fe	2.889		8	4
1.25:1.375:1.375	$Ti_{1.20}Ru_{1.02}Fe_{1.78}$	3.012		8	81
	Ru	2.708	4.271	13	19
1.0:1.5:1.5	$Ti_{1.02}Ru_{0.99}Fe_{1.99}$	3.005		6	74
	Ru	2.705	4.278	15	26

[†]The stoichiometry of that phase was not determined

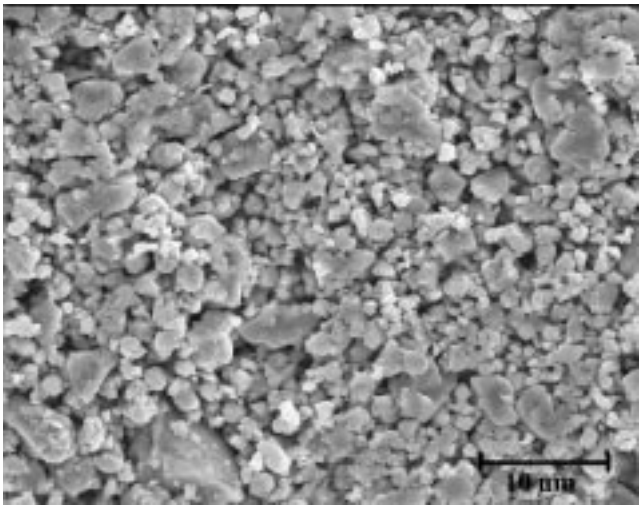

Fig. 2. Scanning electron microscopy micrograph (X2500) of nanocrystalline Ti:Ru:Fe:O (2:1:1:2).

diagrams. A chemical mapping from X-ray fluorescence of Ti, Ru and Fe indicates that these elements are homogeneously dispersed.

3.1.3. *Electrochemical investigations*

We have recently developed an accelerated test to assess the long-term stability in chlorate electrolysis conditions [4]. In this test, the cathode is subjected to a series of alternate cycles of hydrogen discharge (10 min at -250 mA cm^{-2}) and open circuit conditions (10 min). As shown elsewhere [4], in the case of nanocrystalline Ti:Ru:Fe:O (2:1:1:2), this test is more drastic than the one based on continuous electrolysis conditions. Indeed, it was shown that a nanocrystalline Ti:Ru:Fe (2:1:1) electrode falls apart after less than 5 h of OCP/HER cycles while, for the same results, it takes more than 100 h in continuous electrolysis conditions [4].

Nanocrystalline Ti:Ru:Fe:O (2:1:1:w), with $w = 0.0$, 0.5, 1.0, 1.5 and 2.0, were subjected to this accelerated aging test and the variation of the overpotential at -250 mA cm^{-2}, η_{250}, is shown in Figure 4. All these measurements were performed at 70 °C, in the typical chlorate electrolysis conditions defined previously.

We notice that the initial overpotential values of the various materials are very similar (-580 ± 10 mV). This most probably reflects the fact that the surface composition of the material and its chemical state does not show a marked dependency on the bulk O content [8]. The addition of oxygen has, however, a significant influence on the stability of the electrode. In the case of the O-free material, there is a large increase of the overpotential after the twentieth cycle. Such an increase in the overpotential is not observed for the O-containing electrodes. After 50 cycles, all nanocrystalline Ti:Ru:Fe:O (2:1:1:w) with $0.5 \leq w \leq 2.0$ exhibit η_{250} values comprised between -585 mV and -630 mV.

Following the accelerated aging test, the level of deterioration of the various electrodes was estimated by visual inspection of the surface and by measuring the mass loss. These results are summarized in Table 2. In the case of the O-containing materials, there is no mass loss and the surface of the electrode does not show any marked sign of deterioration. In contrast, the electrode made from the O-free material has lost almost all of its electrocatalytic coating.

3.2. *Effect of the Ti content*

3.2.1. *Structural investigations*

The structural analysis of nanocrystalline Ti:Ru:Fe $(2-y:1+y/2:1+y/2)$, with $y = 0.00$, 0.25, 0.50, 0.75 and 1.00 was performed elsewhere [9], through a simultaneous Rietveld refinement analysis of both X-ray and neutron diffraction data. The most relevant structural parameters extracted from this analysis are summarized at the bottom half of Table 1.

The nanocrystalline Ti:Ru:Fe $(2-y:1+y/2:1+y/2)$ are mainly composed of a B2 cubic phase, with minor

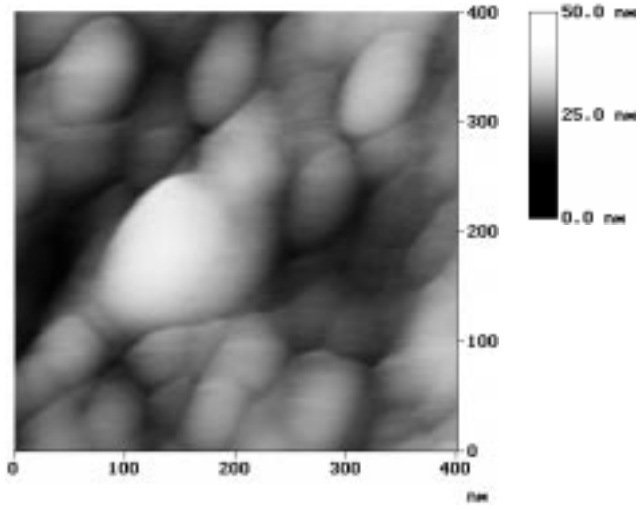

Fig. 3. Atomic force microscopy image of nanocrystalline Ti:Ru:Fe:O (2:1:1:2).

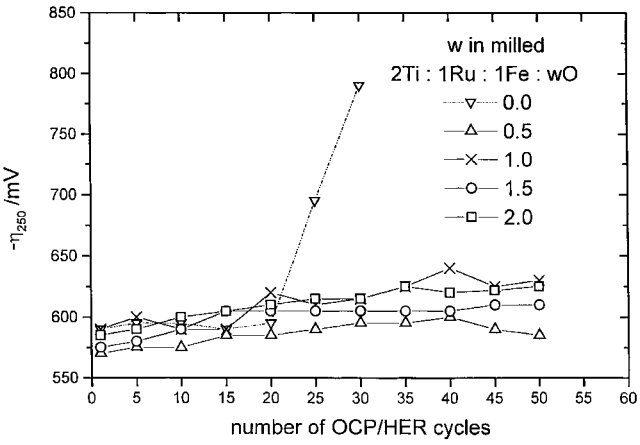

Fig. 4. Variation of the overpotential for the hydrogen evolution reaction at -250 mA cm^{-2} as a function of the number of OCP/HER cycles for various nanocrystalline Ti:Ru:Fe:O (2:1:1:w) materials.

Table 2. Evaluation of the deterioration of the electrodes after an accelerated aging test

Nominal composition	Damaged surface[†]/%	Mass loss/%
Ti:Ru:Fe:O		
2:1:1:0	100	~100
2:1:1:1/2	5	0
2:1:1:1	0	0
2:1:1:3/2	0	0
2:1:1:2	0	0
Ti:Ru:Fe		
2:1:1	100	100
1.75:1.175:1.175	90	67
1.5:1.25:1.25	80	57
1.25:1.375:1.375	20	20
1.0:1.5:1.5	50	43

[†] The figures indicate the percentage of the surface which appear damaged after the test

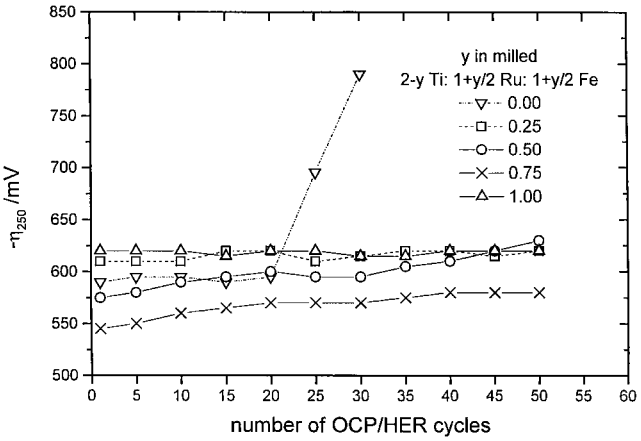

Fig. 5. Variation of the overpotential for hydrogen evolution reaction at −250 mA cm^{-2} as a function of the number of OCP/HER cycles for various nanocrystalline Ti:Ru:Fe $(2-y:1+y/2:1+y/2)$.

phases of Fe and/or Ru. As the titanium content of the initial powder mixture decreases, the proportion of the B2 phase decreases while that of Ru increases. Also, the quantity of Ti atoms incorporated in the B2 phase decreases. As indicated in Table 1, the stoichiometry of the B2 structure changes from $Ti_{1.90}Ru_{1.05}Fe_{1.05}$ to $Ti_{1.02}Ru_{0.99}Fe_{1.99}$ as y in Ti:Ru:Fe $(2-y:1+y/2:1+y/2)$ increases from 0 to 1.0. As shown and discussed elsewhere [9], depletion of Ti atoms from the 1a site of the B2 structure causes this site to be preferentially filled by Fe.

3.2.2. *Morphological and chemical investigations*

The nanocrystalline Ti:Ru:Fe $(2-y:1+y/2:1+y/2)$ powders have a morphology similar to that of nanocrystalline Ti:Ru:Fe:O (2:1:1:*w*), i.e. irregular particles formed by small grains cold welded together. However, we can observe from the SEM images (not shown) that the average particle size of the material increases when the Ti content is reduced. The particle size is typically 1 μm when $y = 0.00$ and 0.25, 2 μm when $y = 0.50$ and 0.75, and 5 μm when $y = 1.0$. These differences in the particle size indicate that the titanium content has a marked effect on the agglomeration/cold welding process during the milling operation. This contrasts with what was previously observed in the case of the Ti:Ru:Fe:O (2:1:1:*w*) materials.

The chemical compositions of nanocrystalline Ti:Ru:Fe $(2-y:1+y/2:1+y/2)$, as determined by EDX analysis, are close to that expected from the nominal composition of the initial powder mixtures. As before, a slight iron enrichment is observed.

3.2.3. *Electrochemical investigations*

Accelerated aging tests were performed on the various nanocrystalline Ti:Ru:Fe $(2-y:1+y/2:1+y/2)$, and Figure 5 displays the overpotential values of the various electrodes at −250 mA cm^{-2}. The initial values for $y = 0.00$, 0.25 and 0.50 are very close to each other at about −580 mV, while the initial overpotential of the compound with $y = 0.75$ is less cathodic ($\eta_{250} =$ −545 mV), and that of the compound with $y = 1.00$ is more cathodic ($\eta_{250} = -620$ mV).

As shown previously, the average particle size and the phase proportion of hcp Ru present in the material varies with the Ti content. For $y = 0.00$, 0.25 and 0.50, the particle size and the proportion of hcp Ru is not much affected by the Ti content, which yields to similar η_{250} values. For $y = 0.75$, the proportion of hcp Ru increases to 19 wt.% and the particle size is close to that of materials with smaller y values. This produces an improvement of the electrocatalytic activity and a reduction (less cathodic) of the η_{250} value. For $y = 1.00$, the phase proportion of hcp Ru reaches 26 wt.%, but the particle size increases also from 2 to 5 μm, thus reducing the effective surface area of the material. That latter factor should affect negatively the overall electrocatalytic activity and could be responsible for the increase in the cathodic overpotential value.

As shown in Figure 5, there is a remarkable improvement in the stability of η_{250} with the number of OCP/HER cycles as soon as y increases above zero. The evaluation of the physical deterioration of the electrodes is summarized in Table 2. All electrodes suffer from some loss of materials. In the case of electrodes with y varying from 0.00 to 0.75, the loss decreases with Ti content. In the case of $y = 1.00$, the damage seems to increase again. However, it must be kept in mind that this material is made of particles with a much larger size than the other compounds, which may have a detrimental effect on the cohesion of the pressed electrode.

In the case of nanocrystalline Ti:Ru:Fe $(2-y:1+y/2:1+y/2)$ with $y > 0.00$, there seems to be a discrepancy between the measurements of η_{250} shown in Figure 5 and the results of Table 2. The former measurements indicate essentially that there is no significant variation of η_{250} over 50 OCP/HER cycles, while the latter shows that there is an appreciable deterioration of these electrodes. This apparent discrepancy arises because the amount of electrocatalysts used in the fabrication of the electrode is larger than the optimum value, this value being defined as the mass of electrocatalyst at

which η_{250} does not vary anymore with additional catalytic powder. Therefore, the evaluation of the mass loss is a more sensitive test than the one based on the measurement of η_{250} for characterizing the stability of the electrodes.

4. Discussion

The stability of nanocrystalline Ti:Ru:Fe (2:1:1) is greatly improved by the addition of oxygen atoms. Indeed, the addition of as little as ~10 at.% of O to the powder mixture, corresponding to Ti:Ru:Fe:O (2:1:1:0.5), is sufficient to change the behavior of the electrode from a non-stable to a stable one. The addition of O atoms above that level does not give rise to further improvements of the stability of the electrode. It is interesting to note that the activity of the nanocrystalline Ti:Ru:Fe:O is not affected by the amount of O introduced in the powder mixture, η_{250} being always in the range of −580 mV.

Likewise, the stability of the nanocrystalline Ti:Ru:Fe materials is effected by the relative proportion of Ti over Ti + Ru + Fe. So, in Ti:Ru:Fe $(2-y:1+y/2:1+y/2)$, varying y from 0.00 to 1.00 leads to a noticeable increase in the stability of the material. However, the stability of the electrode material increases gradually as y varies from 0.00 to 0.75.

The mechanism at the origin of the degradation of the nanocrystalline Ti:Ru:Fe (2:1:1) is well understood. Through a detailed electrochemical study conducted in alkaline solution, it was shown that this material readily absorbs hydrogen during hydrogen discharge and releases it under open-circuit conditions [12]. Also, it was demonstrated through an *in situ* X-ray diffraction study under hydrogen at high pressure that hydrogen absorption is accompanied by a volume expansion of the unit cell of the B2 structure [9]. This process being reversible, the volume of the unit cell goes back to its original value after hydrogen desorption. In the same study, it was also shown that the volume expansion is dependent on the Ti content in the B2 structure [9]. Thus, according to these findings, the increase in stability by reducing the amount of Ti arises because of a change in the hydriding properties of the B2 phase.

Such a change can be understood using Miedema's approach. According to [13], the heat of formation of ternary hydrides AB_nH_{2m}, from the binary intermetallic compound AB_n and gaseous H_2 can be resolved into three contributions

$$\Delta H(AB_nH_{2m}) = \Delta H(AH_m) + \Delta H(B_nH_m) - \Delta H(AB_n) \quad (1)$$

where A is Ti, B stands for a transition metal, and n is assumed to be greater than one. For the purpose of the discussion, and to be able to rely on data already available in the literature, we will consider two limiting cases, namely those where B is either Ru or Fe, and where $m = 3/2$. So, according to [13], the value of ΔH (TiH_2), is −30 kcal mol^{-1} of TiH_2, while those of RuH and FeH are +8 and +4 kcal mol^{-1}, respectively. As expected, the values of ΔH (TiRu) and ΔH (TiFe) are negative. Thus, in the case of TiRu and TiFe, only the first term of Equation 1 is negative and can contribute to the formation of stable ternary hydrides. Thus, in the present study, it does not come as a surprise that the ability of nanocrystalline Ti:Ru:Fe materials to form hydrides decreases as the Ti content of the B2 phase diminishes.

An increase in stability was also observed by adding O to the material. As shown above, the addition of O leads to the formation of titanium oxide phases and the depletion of Ti from the B2 phase. The Ti on the 1a site in the B2 structure is replaced by Fe and Ru atoms. This is similar to the case when Ti:Ru:Fe $(2-y:1+y/2:1+y/2)$ with $y > 0$ are milled together. So, as a first approximation, the increase in stability by either introducing O atoms or by reducing the Ti content has a common origin, namely the formation of Ti-depleted B2 phases which are more resistant to hydriding than Ti_2RuFe.

There are nevertheless some differences between these systems. In the case of Ti:Ru:Fe:O, all materials are equally stable as soon as O is added. However, in the case of Ti:Ru:Fe $(2-y:1+y/2:1+y/2)$, there is a gradual improvement in the stability of the material as the Ti content is reduced. Thus, we observe a large deterioration of the $Ti_{1.5}Ru_{1.25}Fe_{1.25}$ electrode after 50 OCP/HER cycles, whereas the Ti:Ru:Fe:O (2:1:1:1) electrode is intact, despite the fact that the Ti content in the B2 phase of these two materials is roughly the same (see Table 1). One difference between these materials is the presence of oxide phases. Oxides are well known to act as a barrier for H diffusion [14] and, as shown in Table 1, the addition of O to the material leads to the formation of significant amounts of TiO_x (from 6 to 31 wt.%). Thus, it is possible that these oxides could restrict hydrogen absorption when the electrode is cathodically polarized, improving further the long-term stability of the electrode.

In order to test this hypothesis, accelerated aging tests were performed on an electrode made from a mixture of two powders, the first one being the material obtained from milling Ti:Ru:Fe (1.5:1.25:1.25), and the second one being TiO. Two different mixtures where made, namely Ti:Ru:Fe (1.5:1.25:1.25) + 6 wt.% TiO and Ti:Ru:Fe (1.5:1.25:1.25) + 30 wt.% TiO. The deterioration of these composite electrodes at the end of the accelerated aging test (50 cycles of OCP/HER) is similar to that observed on Ti:Ru:Fe (1.5:1.25:1.25) alone. It is clear, however, that the microstructure of that composite material may radically differs from that of nanocrystalline Ti:Ru:Fe:O, and that this change in the microstructure could be at the origin of difference in the stability of the electrodes. Little is known about the microstructural organization of nanocrystalline Ti:Ru:Fe:O and detailed transmission electron microscopy studies would certainly help to resolve some of the issues raised here.

5. Conclusion

The effect of the oxygen and titanium contents on the stability of nanocrystalline Ti–Ru–Fe–O materials prepared by high-energy ball milling and used as activated cathode for the hydrogen evolution reaction in typical chlorate electrolysis conditions has been studied. The main findings are:

(i) In an accelerated aging test, which consists of a succession of HER/OCP cycles, nanocrystalline Ti:Ru:Fe (2:1:1) deteriorates after 10–20 cycles.
(ii) The incorporation of ~10 at.% of oxygen is sufficient to improve the stability of the material to a point where the electrode does not show any sign of deterioration after 50 cycles of HER/OCP.
(iii) There is no change in the activity and stability of the nanocrystalline Ti:Ru:Fe:O materials for [O] varying from 10 to 33 at.%.
(iv) There is some gain in stability by reducing the Ti content in nanocrystalline Ti:Ru:Fe materials.
(v) The level of stability one can get by reducing the Ti content (replacing it by both Fe and Ru) is never as high as that obtained by introducing O atoms in the material.

Acknowledgment

This work was supported by the Natural Sciences and Engineering Research Council of Canada and Hydro-Québec.

References

1. K. Viswanathan and B.V. Tilak, *J. Electrochem. Soc.* **131** (1984) 1551.
2. S. Trasatti, in '*Advances in Electrochemical Science and Technology*' (edited by H. Gerischer and W. Tobias), vol. 2, VCH, New York (1990), p. 1.
3. M. Blouin, D. Guay, J. Huot and R. Schulz, *J. Mater. Res.* **12** (1997) 1492.
4. L. Roué, E. Irissou, A. Bercier, S. Bouaricha, M. Blouin, D. Guay, S. Boily, J. Huot and R. Schulz, *J. Appl. Electrochem.* **29** (1999) 551.
5. A. Van Neste, S.H. Yip, S. Jin, D. Guay, S. Boily and R. Schulz, *Materials Science Forum* **225–227** (1996) 795.
6. M. Blouin, D. Guay, J. Huot, R. Schulz and I.P. Swainson, *Chem. Mater.* **10** (1998) 3492.
7. M. Blouin, D. Guay, S. Boily, A. Van Neste and R. Schulz, *Materials Science Forum* **225–227** (1996) 801.
8. M. Blouin, D. Guay and R. Schulz, *Nanostructured Mater.* **10** (1998) 523.
9. M. Blouin, M.-E. Bonneau, A. Bercier, L. Roué, D. Guay, R. Schulz and I.P. Swainson, *Chem. Mater.* accepted.
10. P.C.S. Hayfield and R.L. Clarke, Proc. Electrochem. Soc. Meeting, Los Angeles, 7–12 May 1989, 87.
11. A.C. Larson and R.B. Von Dreele, 'GSAS-General Structure Analysis System', Los Alamos National Laboratory Report No. LA-UR 86-748 (1986).
12. L. Roué, D. Guay and R. Schulz, *J. Electroanal. Chem.* **455** (1998) 83.
13. A.R. Miedema, K.H.J. Buschow and H.H. Van Mal, *J. Less-Common Met.* **49** (1976) 463.
14. H.H. Lee, K.Y. Lee and J.Y. Lee, *J. Alloys Comp.* **260** (1997) 201.